Signal Processing and Renewable Energy
March 2020, (pp. 77-88)
ISSN: 2588-7327
eISSN: 2588-7335

Retinal Blood Vessel Segmentation Using Gabor Filter and Morphological Reconstruction

Akram Isavand Rahmani[1], Hesam Akbari [2] and Somayeh Saraf Esmaili [3*]

[1] Department of Computer Engineering, Arak University, Arak, Iran.
[2] Department of Biomedical Engineering, Islamic Azad University, South Tehran Branch, Tehran, Iran.
[3] Department of Biomedical Engineering, Islamic Azad University, Garmsar Branch, Garmsar, Iran.

Received: 15-Jan-2020, Revised: 04-Feb-2020, Accepted: 05-Feb-2020.

Abstract

Extraction of blood vessels in retinal images is helpful for ophthalmologists to screen a large number of medical disorders. The changes in the retinal vessels due to pathologies can be easily identified by the retinal vessel segmentation. Therefore, in this paper, we propose an automatic method to extract the blood vessels from various normal and abnormal retinal images. Our proposed method uses the advantages of the optimal Gabor filter and morphological reconstruction to employ robust performance analysis to evaluate the accuracy and sensitivity. Moreover, unsharp filter is used which sharpens the edges of the vessels without increasing noise. Our proposed algorithm proves its better performance by achieving the greatest accuracy, sensitivity, and specificity for the DRIVE and the STARE databases respectively. The results illustrate the superior performance of the proposed algorithm when they compared to other existing vessel segmentation methods.

Keywords: Retinal images; Optimized Gabor filter; Morphological reconstruction; Unsharp Filter.

1. INTRODUCTION

The diagnosis of the fundus image is widely used in many medical diagnoses. Retina images have different and vast applications in security systems and medicine such as human identification and eye disease diagnosis [1]. According to many medical and biometric applications of retinal images, the automatic and accurate extraction of the retinal blood vessels are very important. The analysis of the human retina is a special method which could help ophthalmologists to identify the retinal disease. The disease such as the diabetes, hypertension and arteriosclerosis affect the retina and cause the changes in the retinal blood vessels [2]. The changes in the blood

***Corresponding Author"s Email: s.sesmaeily@iau.garmsar.ac.ir

vessels and the retinal pathology can be identified by segmentation and then analysis of the retinal blood vessels. Some challenges of this research include the existence of a bright region called Optical Disc (OD) and a dark region called Fovea, which are low contrast between vessels and background, and the presence of noise. In most of the previous research, green band of RGB or weighted summations of RGB components in the retinal images have provided a better local contrast between foreground and background [3].

Automatic segmentation of retinal vessels is an important part in the mentioned task. There are various retinal segmentation methods for the retinal vessels' extraction in the fundus images which use two dimensional matched filters and piecewise threshold probing [4,5]. There are several segmentation processes, which use Mumford-Shah model and Gabor wavelet filter [6], Weiner filter and the morphological operations [7]. Authors in [8], present a computerized system for the extraction and quantitative description of the main vascular diagnostic signs from fundus images in hypertensive retinopathy. The features taken into account are vessel tortuosity, generalized and focal vessel narrowing, and presence of Gunn or Salus signs. In [9], vessel segmentation has been performed using Max-Tree to represent the image and branches filtering approach. Mathematical morphology is mostly used for analyzing the shape of the image. In [10], morphological operations have been used to detect the edges and to identify the specific shapes in the image and also to remove the background. In [11], the retinal blood vessels have been extracted by first smoothing the image and then by applying the fuzzy c-means clustering algorithm. In [20], authors proposed a novel method to segment vessel network in fundus image. First vessel centerlines are extracted by using a set of directional line detectors and then an Iterative Geodesic Time Transform (ItGTT) is designed to segment the entire vessel network. The procedure of the ItGTT is to use centerline pixels as the initial reference set and to compute geodesic time between candidate vessel pixels and the reference set iteratively with an adaptive refer-once set updating strategy. The entire vessel network is the binary image of the last reference set at the end of the iteration.

In [21], an innovative methodology has been proposed to detect the vessel tree in retinal angiographies. The automatic analysis of the retinal vessel tree facilitates the computation of the arteriovenous index, which is essential for the diagnosis of a wide range of eye diseases. The results of the detection of arteriovenous structures have been very encouraging, as shown by the system performance evaluation on the available public DRIVE database. An algorithm for vessel segmentation and network extraction in retinal images has been proposed in [22]. A new multi-scale line-tracking procedure starts from a small group of pixels derived from a brightness selection rule and terminates when a cross-sectional profile condition becomes invalid. In [23], the blood vessel segmentation methodologies were tested in two dimensional retinal images acquired from a fundus camera;furthermore, a survey of the techniques has been presented. In [24], a method was proposed for automated segmentation of the vasculature in retinal

images. Based on the pixel feature vectors, the method produces segmentations by classifying each image pixel as vessel or non-vessel. Feature vectors are composed of pixel intensity and two-dimensional Gabor wavelet transform responses taken at multiple scales. The performance of the methods was evaluated on publicly available DRIVE (Staal et al., 2004) and STARE (Hoover et al., 2000) databases of manually labeled images. In [25], a new supervised method for blood vessel detection in digital retinal images has been presented. This method uses a neural network (NN) scheme for pixel classification and computes a 7-D vector composed of gray-level and moment invariants-based features for pixel representation.

In [26], an automatic blood vessel segmentation method starts with the extraction of blood vessel centerline pixels. The final segmentation was obtained by using an iterative region growing method. It merges the binary images from centerline detection part with the images from fuzzy vessel segmentation part. In the proposed algorithm, the blood vessels were enhanced using modified morphological operations and salt and pepper noises were removed from retinal images using Adaptive Fuzzy Switching Median filter. This method has been applied on two publicly available databases, the DRIVE and the STARE and the experimental results were obtained by using green channel images and they were compared with recently published methods. In [27], an automated method for segmentation of blood vessels in retinal images was proposed. A unique combination of techniques for vessel centerlines detection and morphological bit plane slicing was presented to extract the blood vessel tree from the retinal images. The centerlines were extracted by using the first order derivative of a Gaussian filter in four orientations and then the derivative signs and the average derivative values were evaluated. Mathematical morphology has emerged as a proficient technique for quantifying the blood vessels in the retina. The shape and the orientation map of blood vessels were obtained by applying a multidirectional morphological top-hat operator with a linear structuring element followed by bit plane slicing of the vessel enhanced grayscale image. The centerlines were combined with these maps to obtain the segmented vessel tree.

In [28], 2D Gabor wavelet was combined with morphological reconstruction on fundus images to obtain segmented retinal blood vessels. The proposed approach has been validated on sixty color retinal images taken from two databases, i.e. DRIVE and STARE. The accuracy of the proposed approach was up to 95.87%, while on STARE database, the accuracy was 89.46%.

In this paper, a novel algorithm for segmentation of the retinal blood vessels is proposed based on the advantages of the optimal Gabor filter and the morphological reconstruction. Moreover, unsharp filter is used to sharpen the edges of the vessels without increasing noise. By applying this proposed method, the accuracy and sensitivity of the performance is improved.

The structure of this study is as follows. Section 2 covers the explanation of the proposed method including pre-processing, processing and post-processing. Section 3 describes the experimental results and section 4 presents the conclusion of this study.

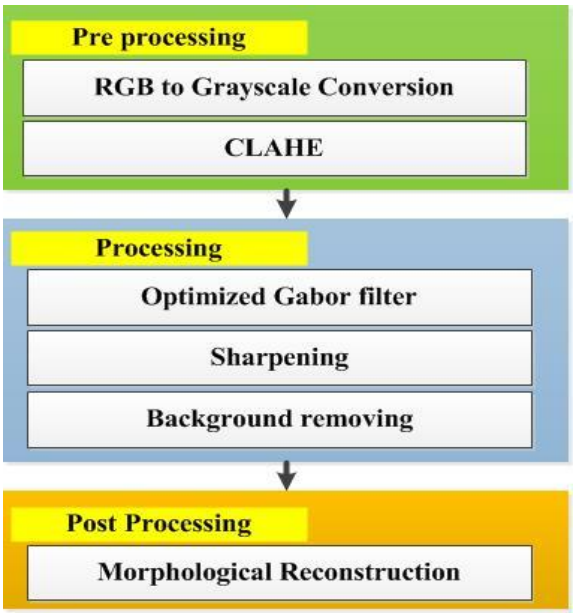

Fig.1. Proposed retinal blood vessel segmentation algorithm.

2. PROPOSED METHOD

Our proposed algorithm consists of three main parts: (A) preprocessing, which includes converting RGB image to grayscale and vessel enhancement using contrast limited adaptive histogram enhancement technique, (B) processing, which uses optimal Gabor filter, unsharp filter and background removing to detect the blood vessels, and (C) post processing, which uses morphological reconstruction to obtain a binary image and finally to define the complete pixels belonging to the retinal vessels. Fig.1 shows the overall procedure of the proposed vessel extraction algorithm.

2.1. Pre-Processing

RGB to Grayscale Conversion: The color fundus image is converted to grayscale image to make the segmentation process easier and to decrease the computational cost. A color image (RGB image) consists of three channels: Red, Green and Blue. Each of these channels is a matrix of $M \times N$ pixels that takes values between 0 and 255[19]. By applying a chromatic filter, we can modify the intensity of each color. The modification criterion depends on the available objects on the image that allows enhancing the areas of interest. For this purpose, we enfeebled the intensity of the red channel pixels, because the ocular background and the blood vessels are very heterogeneous in the red channel in comparison with green and blue channels. Therefore, the red channel is multiplied by the scalar 0.4, while the green and blue channels are multiplied by 1.8 and 2 respectively. Then a grayscale image is obtained using the following weighted average:

$$I=0.4*R+1.8*G+2*B \quad (1)$$

R, G, and B are the values of the pixel in red, green, and blue channels respectively. Fig.2 (a) and (b) shows a sample color image and its grayscale version obtained by applying the chromatic filter [14] respectively.

Image Enhancement using Contrast Limited Adaptive Histogram Equalization (CLAHE): Since thin vessels are very small structures and usually have low local contrast, their segmentation is a hard task. To improve the difference between these thin vessels and the background noise, it is necessary to deepen the contrast of these images and provide a better representation of vessels for the subsequent steps. For this purpose, we used contrast limited adaptive histogram equalization (CLAHE) technique to perform the contrast enhancement [15]. This technique enhances the contrast adaptively across the image by limiting the maximum slope in the transformation function. In histogram

equalization, the dynamic range and contrast of an image is modified by reforming the image such that its intensity histogram has a desired shape [15]. This is obtained by using cumulative distribution function as the mapping function. The intensity levels are modified such that the peaks of the histogram are stretched and the troughs are compressed. If a digital image has N pixels distributed in L discrete intensity levels and n_k is the number of pixels with intensity level i_k, then the probability density function (PDF) of the image is described by equation (2) as:

$$f_i\ (i_k\ ) = \frac{n_k}{N} \tag{2}$$

The cumulative density function (CDF), F_k, is defined in equation (3):

$$F_k(i_k) = \sum_{j=0}^{k} f_i(i_j) \tag{3}$$

Because the gray values are far apart from each other in the image, the histogram equalization cannot return suitable modified values in myocardial nuclear images. To solve this problem, CLAHE technique cuts the histogram at some threshold and then equalization is applied adaptively to small data regions called tiles rather than the whole image. The resulting neighboring tiles are then stitched back seamlessly using bilinear interpolation [15]. The contrast in the homogeneous region can be limited so that noise can be avoided. Fig.2(c) represents the vessel enhanced image obtained by the CLAHE technique.

2.2. Processing

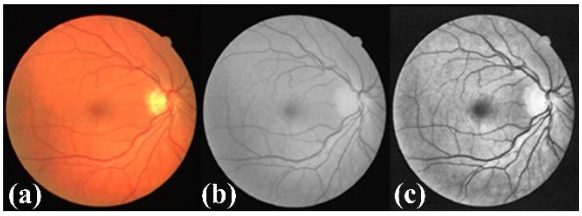

Fig.2. a) Original RGB image b) gray scale image c) Vessel enhanced image using CLAHE.

Here we used optimized Gabor filter [16, 17] to detect the blood vessels in retinal images. The Gabor filters are a set of orientation and frequency sensitive band pass filters, which have the optimal localization in both the frequency and spatial contents of the patterns.

Optimized Gabor filter: The optimized Gabor filter kernels are sinusoidally modulated:

$$\sigma_x = k \tag{4}$$

$$\sigma_y = \frac{\sigma_x}{\gamma} \tag{5}$$

$$x_\theta = x\cos\theta + y\sin\theta \tag{6}$$

$$y_\theta = -x\sin\theta + y\cos\theta \tag{7}$$

$$g_\theta(x,y) = \exp\{-\frac{1}{2}(\frac{x_\theta^2}{\sigma_x} + \frac{y_\theta^2}{\sigma_y})\}\cos(2\pi fx) \tag{8}$$

Here σ_x is the standard deviation in direction x along the Gaussian filter that determines the bandwidth of the filter. σ_y ,is the standard deviation across the Gaussian filter that controls the orientation selectivity of the filter. The parameter f is the central frequency of pass band and θ is orientation of the filter. The angle of zero gives the filter response to a vertical feature. Here σ_x and

σ_y were set to 1.5, f was equal to 2, and θ was considered $\pi/2$ or 90°. By convolving an optimized Gabor function $g_\theta(x,y)$ with image patterns, we can evaluate their similarities. The optimized parameters are derived by taking into account the detected size of line structures. By applying Gabor filter to each pixel, the response will be a complex number. If the real and imaginary parts are denoted by *Re* and *Im* respectively, then the feature vector is obtained using local energy as follows:

$$I_{out} = \sqrt{Im^2(x,y) + Re^2(x,y)} \qquad (9)$$

The optimal Gabor filter is applied on the enhanced images (obtained from the preprocessing step). Fig. 3 represents the resulting image after applying optimized Gabor filter to the enhanced image in Fig. 2(c).

Sharpening: In this phase, the resulting image of the previous step is sharpened to enhance the appearance of edges, which represent vessels. We used an unsharp mask [18], which is a simple sharpening operator that derives its name from the fact that it enhances edges by subtracting an unsharp or smoothed version of an image from the original image:

$$g(x,y) = f(x,y) - f_{smooth}(x,y) \qquad (10)$$

in which $f_{smooth}(x,y)$ is the smoothed version of $f(x,y)$. This edge image can be used for sharpening if we add it to the original signal:

$$f_{sharp}(x,y) = f(x,y) + k * g(x,y) \qquad (11)$$

Here k is the scaling contrast and it was set to one. We used the unsharp filter by returning

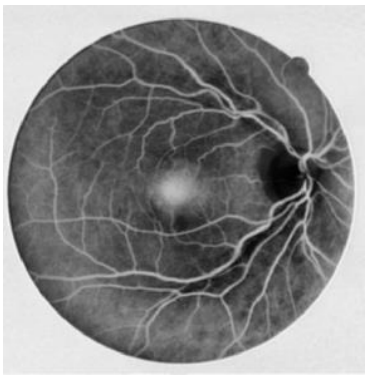

Fig.3. Optimized Gabor filtered image.

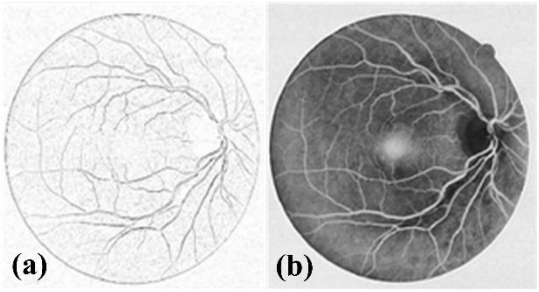

Fig.4. a) The edge image b) Contrast enhanced image after sharpening.

a 3-by-3 unsharp contrast enhancement that uses the negative of the Laplacian Gaussian filter (which its central peak is negative) with parameter alpha to highlight vessel edges in the image obtained from the previous step. Alpha controls the shape of the Laplacian and must be in the range of 0 to 1. This amount determines the strength of the sharpening and it was set to one. The advantages of the above sharpening method are its simplicity and the fact that the sharpening is done without increasing noise.

Fig 4 (a) and (b) represent the edge image and the contrast enhanced image after applying the sharpening respectively.

Background removing: After sharpening the image, we uniformed the background of the images to obtain a suitable vessel segmented image. This task meant to remove the gray

level deformation by subtracting an estimated background image from the original grayscale image. Therefore, we used a 30×30 median filter to estimate the approximate background from the previous image. Then by subtracting the median filter response from the previous image, the blood vessels were presented brighter than the background [10].

2.3. Post Processing

Morphological Reconstruction: In this part, we used a region growing algorithm to reconstruct true vessel pixels. More importantly, for most cases, the images in gray levels are defined so that the gray level intensity at each pixel is an integer value belonging to the natural range [0,255]. However, the normalized images have several advantages to represent a better contrast enhancement in the images and they turn out to be a useful tool for their segmentation. Therefore, the morphological operators can gain a far better result when they are applied to normalized images. We used normalized images for the last step of our proposed algorithm. The normalization function was considered as below:

$$f(I) = x_{ij} / (\max(x_{11}, x_{12}, ..., x_{mn})) \quad (12)$$

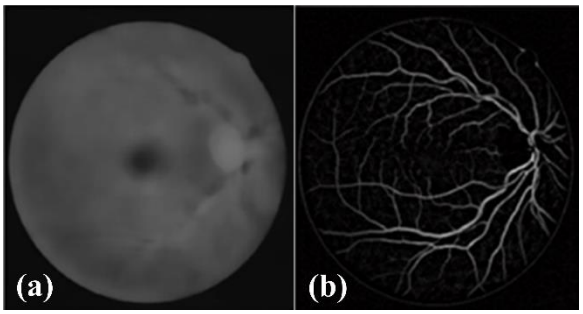

Fig. 5. (a) and (b) represent the estimated background and the background removed image as an illustration respectively.

in which I represents the matrix with $M \times N$ pixels of the image, and x_{ij} denotes each pixel of the image and the denominator calculates maximum intensity in the image.

After normalization, we selected the binary morphological reconstruction method as a thresholding method, which was applied to the previous retinal image. By applying the threshold, the background was eliminated and the properly segmented binary image of the retinal vessel was obtained. Morphological reconstruction [19] involves two images and one structuring element. One image, the marker, contains the starting points for the transformation. The other image, the mask, constrains the transformation. The structuring element is used to define connectivity. Here the morphological reconstruction uses the concept of geodesic dilation by considering 8-connected neighborhoods for 2-D binary images.

Let R denote the marker image, G the mask image, and B the structuring element. Both of the images are binary images and R $\subseteq$ G. The geodesic dilation of size 1 of the marker image with respect to the mask, denoted by $D_G^1(R)$, is defined as follows:

$$D_G^1(R) = (R \oplus B) \bigcap G \quad (13)$$

here $\bigcap$ means the set intersection and is interpreted as a logical AND. The geodesic dilation of size n of R with respect to G is defined as follows:

$$D_G^{(n)}(R) = D_G^{(1)}(D_G^{(n-1)}(R)) \quad (14)$$

In this recursive phrase, the set intersection in equation 12 is performed at each step. Note that the reconstructed image

in this case is very similar to the mask image although it has much less noise.

Fig.6 shows the marker and mask images and the output image of the morphological reconstruction operator. The result obtained by morphological reconstruction illustrates the superior performance of the reconstruction when it compared to a simple thresholding operation, represented in this figure by the mask image.

3. EXPERIMENTAL RESULT

In order to implement and test the proposed method, the employed computer had the following specifications: Windows 10, 64-bit, Intel Core i7-4720 CPU @ 2.60 GHz, 8 GB memory. The used software was MATLAB R2018a. However, we used fundus images provided by two public databases, the DRIVE [12] and the STARE [13]. The DRIVE database consists of 40 color fundus photographs from which, seven images contain pathologies, namely exudates, hemorrhages and pigment epithelium changes. The other database, STARE contains 20 images for blood vessel segmentation and ten of them contain pathologies. Some examples of the segmented images from DRIVE and STARE databases using our proposed segmentation algorithm are shown in Fig.7 and Fig.8.

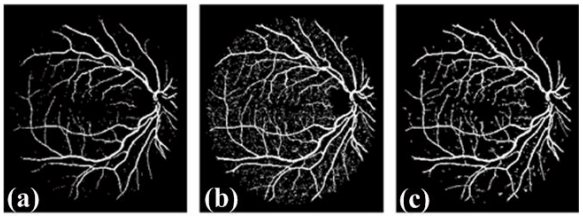

Fig.6.a) Marker image b) Mask image c) Reconstructed image.

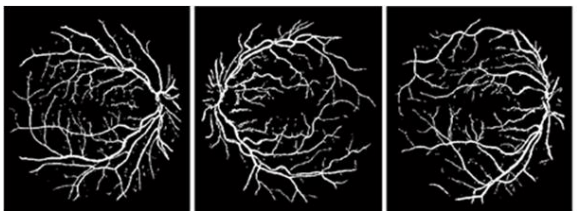

Fig.7. Three examples of segmented images from DRIVE database.

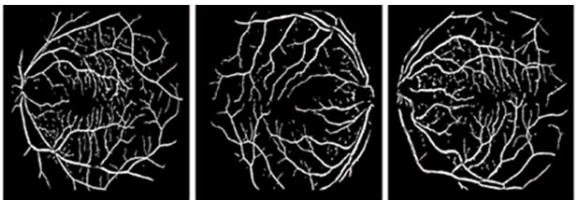

Fig.8. Three examples of segmented images from STARE database.

The evaluation results are given as the pixel-wise sensitivity, specificity, and accuracy of all the segmentation compared to the ground truth, where sensitivity is a normalized measure of true positives, specificity measures the proportion of true negatives, and accuracy represents the proportion of the total number of correctly classified pixels related to the total number of pixels.

In the following equations, true positive (TP) is the number of blood vessels correctly detected, false positive (FP) is the number of non-blood vessels which are detected wrongly as blood vessels, false negative (FN) is the number of blood vessels that are not detected and true negative (TN) is the number of non-blood vessels which are correctly identified as non-blood vessels.

$$Accuracy = TP+TN / TP+TN+FP+FN \quad (15)$$

$$Sensitivity = TP / TP+FN \quad (16)$$

$$Specificity = TN / TN+FP \quad (17)$$

Tables 1 and 2 illustrate the average percentage of accuracy, sensitivity, and specificity for different methods on the DRIVE and STARE databases respectively. Comparisons based on DRIVE database indicate that our proposed algorithm has the highest accuracy and sensitivity compared to all other listed methods. In addition, our proposed method has the highest specificity compared to [21], [22], [24] and [25].

Comparing the methods on the STARE database illustrates that our proposed algorithm has the highest accuracy, sensitivity and specificity compared to [28] and [29] methods. Moreover, it has the highest accuracy, sensitivity in comparison with [5] and is equal to specificity in [27]. Comparison of the proposed method and listed approaches based on DRIVE and STARE databases are shown in Table I and Table II respectively.

Therefore, our proposed vessel extraction technique has consistent performance in both normal and abnormal images compared to other listed approaches. Hence, eye care specialists can potentially monitor larger populations using this algorithm. Our segmentation method could obtain accuracy, sensitivity, and specificity values of 95.21%, 74.00 and 97.26 for the DRIVE database and 95.37, 79.66 and 96.80 for the STARE database respectively.

4. CONCLUSION

In this paper, a simple algorithm for retinal blood vessel segmentation was proposed. This method was based on optimal Gabor filter and morphological reconstruction. Our proposed vessel extraction technique has consistent performance in both normal and

Table 1. ***Average percentage of performance measurements for different methods on DRIVE database.***

Method	Accuracy (%)	Sensitivity (%)	Specificity (%)
Dai, [20]	94.60	70.91	98.06
Espona, [21]	93.16	66.34	96.82
Vlachos, [22]	92.85	74.68	95.51
Fraz, [23]	94.30	71.52	97.68
Soares, [24]	93.16	66.34	96.82
Diego Marin, [25]	94.52	70.67	96.01
R Akhavan, [26]	95.13	72.52	97.33
Proposed Method	95.21	74.00	97.26

Table 2. ***Average percentage of performance measurements for different methods on STARE database.***

Method	Accuracy (%)	Sensitivity (%)	Specificity (%)
Fraz, [27]	94.42	73.11	96.80
Hoover, [5]	92.62	67.51	95.67
Marin, [25]	95.26	69.44	95.19
Adi, [29]	89.46	78.74	90.45
proposed method	95.37	79.66	96.80

abnormal images. To validate the proposed method, we used images provided by two public databases, namely DRIVE and STARE. We could achieve the greatest accuracy, sensitivity, and specificity values of 95.21%, 74.00% and 97.26% for the DRIVE database and 95.37, 79.66, and 96.80 for the STARE database respectively.

Our proposed vessel extraction technique does not require any user intervention and it has consistent performance in both normal and abnormal images.

REFERENCES

[1] Y. Jiang, H. Zhang, N.Tan and L.Chen, “Automatic Retinal Blood Vessel Segmentation Based on Fully Convolutional Neural Networks”, International Journal of Computer Science and Engineering,vol.11,No. 1112,pp.1-22, Symmetry 2019.

[2] N. Memari, A.Ramli, M.Saripan, S.Mashohor, M.Moghbel,“Retinal Blood Vessel Segmentation by Using Matched Filtering and Fuzzy C-means Clustering with Integrated Level Set Method for Diabetic Retinopathy Assessment”, Journal of Medical and Biological Engineering,vol.39,pp.713-731,2019.

[3] P. Nazari, H. Pourghassem, “An Automated Vessel Segmentation Algorithm in Retinal Images Using 2D Gabor Wavelet”, 8th Iranian Conference on Machine Vision and Image Processing (MVIP2013), pp. 145-149, Zanjan, Iran, 10-12 Sep. 2013.

[4] S. Chaudhuri, S. Chatterjee, N. Katz, M. Nelson, and M. Goldbaum, "A Review On Retinal Blood Vessel Segmentation Methodologies”, INTERNATIONAL JOURNAL OF SCIENTIFIC & TECHNOLOGY RESEARCH, vol. 9, pp. 738-747, July 2012.

[5] B. Sumathy, S. Poornachandra, "Retinal Blood Vessel Segmentation using Morphological Structuring Element and Entropy Thresholding," 2, Coimbatore, India, IEEE Transactions,2019.

[6] X. Du and T. D. Bui, "Retinal image segmentation based on Mumford-Shah model and Gabor wavelet filter," in Pattern Recognition (ICPR), 2010 20th International Conference on, pp. 3384-3387, 2010.

[7] L.TRAN ," IMAGE Processing Course Project: Image Filtering with Wiener Filter and Median Filter," Advanced Image Processing Course , April 2019.

[8] M. Foracchia, E. Grisan, and A. Ruggeri, "Extraction and quantitative description of vessel features in hypertensive retinopathy fundus images," in Book Abstracts 2nd International Workshop on Computer Assisted Fundus Image Analysis, p.6, 2001.

[9] Y. Yang, S. Huang, and N. Rao, "An automatic hybrid method for retinal blood vessel extraction," International Journal of Applied Mathematics and Computer Science, vol. 18, pp. 399-407, 2008.

[10] N. Patton, T. M. Aslam, T. MacGillivray, I. J. Deary, B. Dhillon, R. H. Eikelboom, et al., "Retinal image analysis: concepts, applications and

potential," Progress in retinal and eye research, vol. 25, pp. 99-127, 2006.

[11] K. Noronha, J. Nayak, and S. Bhat, "Enhancement of retinal fundus Image to highlight the features for detection of abnormal eyes," in TENCON 2006. 2006 IEEE Region 10 Conference, pp. 1-4, 2006.

[12] M. Niemeijer, J.J. Staal, B.v. Ginneken, M. Loog, M.D.Abramoff, DRIVE: digital retinal images for vessel extraction,http://www.isi.uu.nl/Research/Databases/DRIVE,2004.

[13] A. Hoover, V. Kouznetsova, and M. Goldbaum, "Locating blood vessels in retinal images by piecewise threshold probing of a matched filter response," Medical Imaging, IEEE Transactions on, vol. 19, pp. 203-210, 2000.

[14] J. Gasparri, A. Bouchet, G. Abras, V. Ballarin, and J. Pastore, "Medical Image Segmentation using the HSI color space and Fuzzy Mathematical Morphology," in Journal of Physics: Conference Series, p. 012033 , 2011.

[15] C. Kumar, R. Aruna, " Contrast Limited Adaptive Histogram Equalization (Clahe) Based Color Contrast and Fusion for Enhancement of Underwater Images," Journal of Engineering (IOSRJEN), vol.5, pp.63-69,2018.

[16] A. Kugaevskikh, " Comparison Gabor Filter Parameters for Efficient Edge Detection", International Journal Of Computer Vision, August 2017.

[17] S. K. Kuri and M. Hossain, "Automated retinal blood vessels extraction using Optimized Gabor filter," in Informatics, Electronics & Vision (ICIEV), 2014 International Conference on, pp. 1-5, 2014.

[18] R. C. Gonzalez and R. E. Woods, " Improving the Sharpness of Digital Image Using an Amended Unsharp Mask Filter " , International Journal of Image, Graphics and Signal Processing,vol.3, pp.1-9,March 2019.

[19] B .Biswal, T. Pooja, N. Subrahmanyam, "Robust retinal blood vessel segmentation using line detectors with multiple masks", IET Image Processing,vol.12,No.3,2018.

[20] B. Dai, W. Bu, X. Wu, and Y. Teng, "Retinal vessel segmentation via Iterative Geodesic Time Transform," in Pattern Recognition (ICPR), 2012 21st International Conference on, pp. 561-564, 2012.

[21] L. Espona, M. J. Carreira, M. Ortega, and M. G. Penedo, "A snake for retinal vessel segmentation," in Pattern Recognition and Image Analysis, ed: Springer, pp. 178-185, 2007.

[22] M. Vlachos and E. Dermatas, "Multi-scale retinal vessel segmentation using line tracking," Computerized Medical Imaging and Graphics, vol. 34, pp. 213-227, 2010.

[23] M. M. Fraz, P. Remagnino, A. Hoppe, B. Uyyanonvara, C. G. Owen, A. R. Rudnicka, et al., " Blood vessel segmentation methodologies in retinal images--a survey",vol. 25, pp. 407-433, Elsevier, 2012.

[24] J. V. Soares, J. J. Leandro, R. M. Cesar, H. F. Jelinek, and M. J. Cree, "Retinal vessel segmentation using the 2-D Gabor wavelet and supervised classification," Medical Imaging,IEEE

Transactions on, vol. 25, pp. 1214-1222, 2006.

[25] D. Marín, A. Aquino, M. E. Gegúndez-Arias, and J. M. Bravo, "A new supervised method for blood vessel segmentation in retinal images by using gray-level and moment invariants-based features," Medical Imaging, IEEE Transactions on, vol. 30, pp. 146-158, 2011.

[26] R. Akhavan and K. Faez, "A Novel Retinal Blood Vessel Segmentation Algorithm using Fuzzy segmentation, " International Journal of Electrical and Computer Engineering (IJECE) , vol. 40,No.4, pp. 561-572, 2014.

[27] M. M. Fraz, S. Barman, P. Remagnino, A. Hoppe, A. Basit, B. Uyyanonvara, et al., "An approach to localize the retinal blood vessels using bit planes and centerline detection," Computer methods and programs in biomedicine, vol. 108, pp. 600-616, 2012.

[28] H. Adi Nugroho, T. Lestari, R. Amalia Aras, I. Ardiyanto, "Segmentation of Retinal Blood Vessels Using Gabor Wavelet and Morphological Reconstruction," 3rd International Conference on Science in Information Technology, pp. 513-516, 2017